ЖУРНАЛ СТРУКТУРНОЙ ХИМИИ

2017. Том 58, № 7 *Сентябрь – октябрь* *С. 1327 – 1335*

UDC 541.6

PROBING THE ELECTRONIC STRUCTURE AND AROMATICITY IN $W_3F_3^{+/-}$, W_3F_3X (X = Li, Na, K), AND $W_3F_3Y^+$ (Y = Be, Mg, Ca) CLUSTERS

Q. Jin[1], B. Jin[2], F.K. Jin[3]

[1]*School of Chemical Engineering, Beijing Institute of Petrochemical Technology, Beijing, P. R. China*
E-mail: jinqiao@bipt.edu.cn
[2]*School of Environment and Biology Engineering, Shenyang University of Chemical Technology, Shenyang, P. R. China*
[3]*Liaoning University of Petroleum and Chemical Technology, Fushun, P. R. China*

Received July, 28, 2015 *Revised — August, 29, 2015*

The equilibrium geometries, electronic properties, and aromaticity of tungsten low-fluoride $W_3F_3^{+/-}$ clusters and their half-sandwich-type W_3F_3X (X = Li, Na, K) and $W_3F_3Y^+$ (Y = Be, Mg, Ca) complexes are investigated by density functional theory (DFT) methods. The calculations reveal three types of the *d* bonding interaction existing in the planar regular hexagonal $W_3F_3^+$ (D_{3h}, $^1A_1'$) cation, $W_3F_3^-$ (D_{3h}, $^3A_1''$) anion, and W_3F_3X (C_s, $^3A''$) (X = Li, Na, K), $W_3F_3Y^+$ (C_s, $^3A''$) (Y = Be, Mg, Ca) complexes. The δ aromaticity is revealed in the $W_3F_3^+$ (D_{3h}, $^1A_1'$) cation, while the $W_3F_3^-$ (D_{3h}, $^3A_1''$) anion possesses partial δ aromaticity. They have two delocalized δ electrons, satisfying the (4*n*+2) Hückel electron counting rule.

DOI: 10.26902/JSC20170704

K e y w o r d s: tungsten low-fluoride cluster, δ aromaticity, DFT calculation.

INTRODUCTION

Aromaticity was introduced into chemistry by Kekule. This concept was originally accepted and established in organic chemistry to describe the delocalized π bonding in planar, cyclic, and conjugated molecules possessing (4*n*+2) π electrons [1]. In recent years, it has been extended to the realm of all-metal clusters, then later to main-group element and transition-metal clusters [2—16]. It was shown that the prototypical all-metal aromatic cluster Al_4^{2-} was an example of a doubly aromatic system with the simultaneous presence of σ radial (σ_r), σ tangential (σ_t), and π aromaticites. In recent years, much attention has been given to aromaticity and antiaromaticity of transition metal clusters and complexes with the multiple charge [17—25]. The presence of *d* orbitals endows much more diverse chemistry, structures, and chemical bonding to transition metal clusters and compounds which exhibit physical and chemical properties. The delocalized multi-center bonding in the transition metal systems also raises the interesting possibility for *d* orbital aromaticity, in particular, δ aromaticity, which has been actively pursued lately [26—33]. In 1964, Cotton and co-workers published a research report [34] in which the presence of a new type of the chemical bond, which is a δ bond between two Re atoms of $K_2[Re_2Cl_8]\cdot 2H_2O$, was shown. Until 2007, the first circularly delocalized three-center δ bond was observed for $Ta_3O_3^-$ (D_{3h}, $^1A_1'$) in a joint photoelectron spectroscopy (PES) and *ab initio* studies of

Zhai et al. [32]. The totally delocalized multi-center δ bond renders δ aromaticity for $Ta_3O_3^-$ and represents a new mode of chemical bonding, having a meaning of a milestone. $Ta_3O_3^-$ is the first δ aromatic molecule confirmed experimentally and theoretically. This report suggests that δ aromaticity exists in many multinuclear low-oxidation-state transition metal compounds. In the same year, Averkiev and Boldyrev [33] theoretically predicted that the Hf_3 cluster in the (D_{3h}, $^1A_1'$) ($1a_1'^2 2a_1'^2 1e'^4 1a''^2_2 3a_1'^2$) state possessed triple (σ, π, and δ) aromaticity. At present, systems containing transition metal clusters have been actively studied by experiments and theory in chemistry and biochemistry. The number of all transition metal aromatic/antiaromatic clusters and compounds reported in the literature has grown enormously: Cu_3^+ [35], X_3^- (X = Sc, Y, La) [36], X_3^{2-} (X = Zn, Cd, Hg) [10], Hf_3 [33], Ta_3^- [37], $M_3O_9^-$ and $M_3O_9^{2-}$ (M = W, Mo) [39], $Ta_3O_3^-$ [32, 39], $Ta_3O_x^-$ (x = 1—8) [39], Nb_3^- and $Nb_3O_n^-$ (n = 1—8) [40], Re_n ($n \le 8$) [41], Re_3X_9 and $Re_3X_9^{2-}$ (X = Cl, Br) [42, 43], $Re_3X_9^{2-}$ (X = Cl, Br) [44], M_3O_8 and $M_3O_8^-$ (M = Cr, W) [45], $M_3O_9^-$ and $M_3O_9^{2-}$ (M = W, Mo) [46], $W_3^{0/-/2-}$ and $W_3O_x^{-/0}$ (x = 0—2) [47]. Obviously, transition metal compounds contain mainly rich-oxidation-state and low-oxidation-state transition metal compounds. We consider that δ aromaticity also may exist in other multi-nuclear transition metal clusters. The $W_3F_3^{+/-}$ clusters were derived from low-fluoride transition metal clusters, and this drives the objective to be achieved at the DFT level.

COMPUTATIONAL METHODS

All calculations were performed using the Gaussian 03 program package [48]. Equilibrium geometries and vibrational frequencies of the $W_3F_3^{+/-}$ cluster, the half-sandwich-type W_3F_3X (X = Li, Na, K) and $W_3F_3Y^+$ (Y = Be, Mg) complexes were fully optimized by the hybrid DFT-B3LYP method [50, 51]. For $W_3F_3^{+/-}$, W_3F_3X (X = Li, Na, K), and $W_3F_3Y^+$ (Y = Be, Mg, Ca) clusters, they were optimized at B3LYP levels of theory with the 6-311++G* basis set for F, Li, Na, K, Be, Mg, Ca and the LANL2DZ basis set for heavier W metal (Z = 74). Vibrational frequencies were calculated by the B3LYP methods to characterize the stationary points as minima (number of imaginary frequencies N_{imag} = 0) or transition states (N_{imag} = 1) and the second-order saddle point (N_{imag} = 2). Molecular orbitals (MOs) of the most stable $W_3F_3^{+/-}$ cluster, the half-sandwich-type W_3F_3Li (C_s, $^3A''$) and $W_3F_3Be^+$ (C_s, $^3A''$) complexes were calculated by the B3LYP method with the corresponding basis set. All MO pictures were made using the Gaussview 3.7 program [48]. The bonding nature and atomic charge were analyzed by the natural bond orbital (NBO) analysis [52] using the B3LYP method with the corresponding basis set.

RESULTS AND DISCUSSION

The optimized geometric structures for the global minimum of $W_3F_3^{+/-}$ and selected low-lying isomers are illustrated in Fig. 1. The relative energies (ΔE) and the number of imaginary frequencies (N_{imag}), the lowest vibrational frequencies (γ_{min}), and W—W and W—F bond lengths (in Å) for the $W_3F_3^{+/-}$ isomers are given in Table 1. The optimized geometric structures for the global minimum of the half-sandwich-type W_3F_3X (X = Li, Na, K), $W_3F_3Y^+$ (Y = Be, Mg, Ca) complexes are illustrated in Fig. 2. Table 1 lists the number of imaginary frequencies (N_{imag}), the lowest vibrational frequencies (γ_{min}), the relative energies (ΔE), the Wiberg bond index (WBI) of W—W ($WBI_{W—W}$), W—F ($WBI_{W—F}$), and total WBI of metal centers M (WBI_M), the natural atomic charges Q_M of the metal atom, HOMO energies (E_{HOMO}), HOMO-LUMO energy gaps (ΔE) at the B3LYP level for W_3F_3X (X = Li, Na, K) and $W_3F_3Y^+$ (Y = Be, Mg, Ca). The MOs pictures for the most stable $W_3F_3^+$ (D_{3h}, $^1A_1'$) cation, the $W_3F_3^-$ (D_{3h}, $^3A_1'$) anion, and the half-sandwich-type W_3F_3Li (C_s, $^3A''$), $W_3F_3Be^+$ (C_s, $^3A''$) complexes are illustrated in Fig. 3.

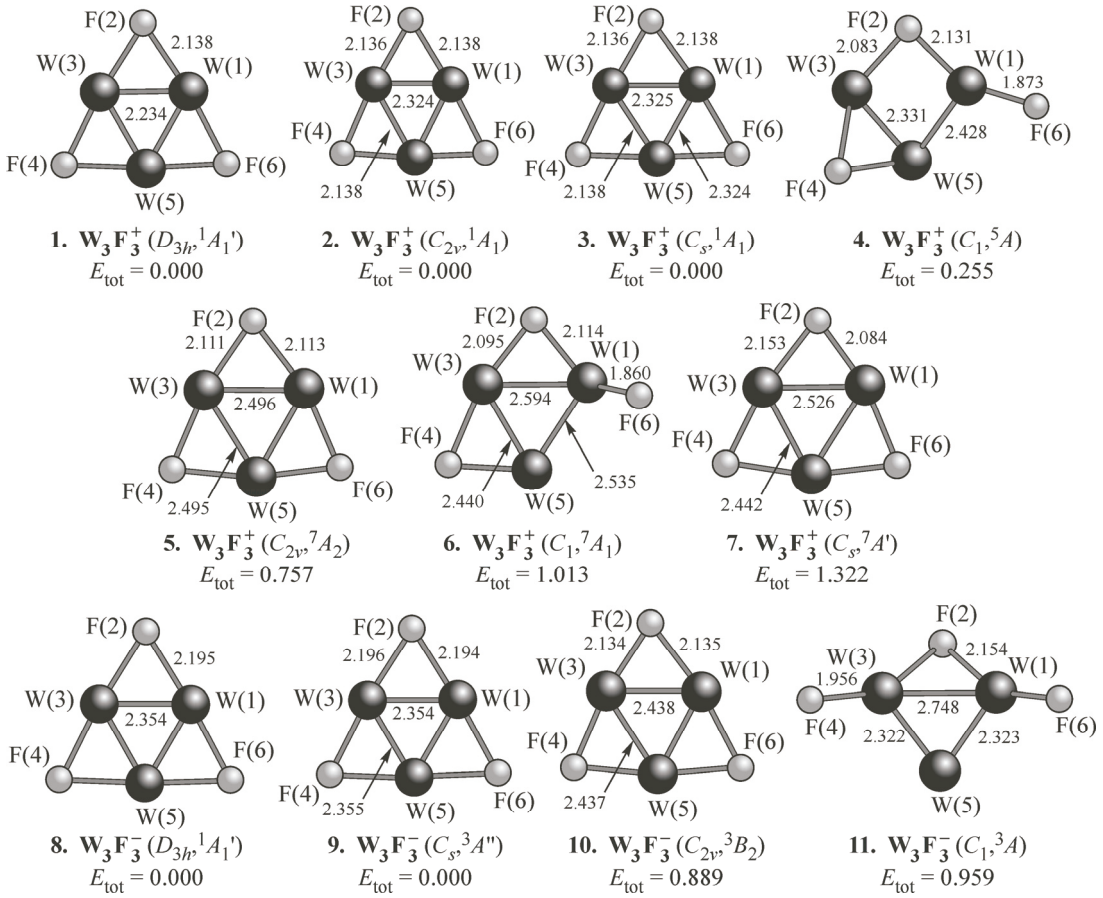

Fig. 1. Optimized structures for the global minimum of $W_3F_3^+$ (D_{3h}, $^1A_1'$), $W_3F_3^-$ (D_{3h}, $^3A_1'$), and their selected low-lying isomers. The relative energies ΔE_{tot} (kcal/mol^{-1}) and interatomic distances (Å) were calculated at the B3LYP/LANL2DZ level of theory

$W_3F_3^+$ (D_{3h}, $^1A_1'$) and $W_3F_3^-$ (D_{3h}, $^3A_1'$) clusters. Geometric structures. Firstly, we performed an extensive search for the $W_3F_3^{+/-}$ global minimum for the singlet, triplet, quintet, and heptet states at the B3LYP level of theory with the corresponding basis set.

For the single charged $W_3F_3^{+/-}$ cluster, we considered all different geometries and spin multiplicities. A selected set of optimized low-lying structures and electronic states for $W_3F_3^{+/-}$ are summarized in Fig. 1, along with their equilibrium geometries and relative energies. For the $W_3F_3^+$ cation seven geometric isomers were obtained, which had different symmetry, i.e. structures **1**, **2**, **3**, **4**, **5**, **6**, and **7** (Fig. 1). Seven geometric isomers of $W_3F_3^+$ with different spins are minima on the B3LYP potential energy surfaces with all real vibrational frequencies. The theoretical studies show that the $W_3F_3^+$ global minimum has a planar regular hexagonal structure **1** D_{3h} ($^1A_1'$) (Fig. 1). Therefore, the ground state of $W_3F_3^+$ is found to be a singlet state $^1A_1'$ with the D_{3h} symmetry and a W—W bond length of 2.324 Å. Our theoretical results clearly show that $W_3F_3^+$ has a propensity to adopt a singlet D_{3h} ($^1A_1'$) ground state, whereas two nearly isoenergetic states C_{2v} ($^1A_1$) and C_s ($^1A'$) are found to compete for the ground state of $W_3F_3^+$; they are singlet states at the B3LYP level of theory with the corresponding basis set. A completely distorted pentagon structure C_1 (^5A) with a quintet state for $W_3F_3^+$ (Fig. 1, **4**) is found to be only 0.255 eV above the ground state. This C_1 (^5A) structure has one terminal and one

Table 1

Calculated number of imaginary frequencies (N_{imag}), *lowest vibrational frequencies* (γ_{min}) (cm^{-1}), *Wiberg bond index* (WBI) *of* W—W ($WBI_{W—W}$), W—F ($WBI_{W—F}$), *and total* WBI *of metal centers* M (WBI_M), *natural atomic charges* Q_M (e) *of the metal-atom bond*, HOMO *energies* (E_{HOMO}) (eV), HOMO-LUMO *energy gaps* (ΔE) (eV) *at the* B3LYP/ LANL2DZ *level for* W_3F_3X (C_s, $^3A''$) (X = Li, Na, K) *and* $W_3F_3Y^+$ (C_s, $^3A''$) (Y = Be, Mg, Ca)

Species	N_{imag}	γ_{min}	$WBI_{W—W}$	$WBI_{W—F}$	WBI_M	Q_M	E_{HOMO}	ΔE
W_3F_3Li (C_s, $^3A'_1$)	0	207	1.963	0.277	0.334	0.8128	–0.22202	0.22122
W_3F_3Na (C_s, $^3A'_1$)	0	74	1.968	0.273	0.346	0.8054	–0.18672	0.18420
W_3F_3K (C_s, $^3A'_1$)	0	55	1.988	0.270	0.204	0.8913	–0.20267	0.19728
$W_3F_3Be^+$ (C_s, $^3A_1$)	0	131	1.685	0.316	1.295	1.1521	–0.46008	0.30532
$W_3F_3Mg^+$ (C_s, $^3A_1$)	0	41	1.832	0.307	0.956	1.2976	–0.47347	0.30907
$W_3F_3Ca^+$ (C_s, $^3A_1$)	0	62	1.874	0.298	0.222	1.5293	–0.41652	0.36592
$W_3F_3^-$ (D_{3h}, $^3A'_1$)	0	99	2.108	0.256			–0.02755	0.15903
$W_3F_3^-$ (D_{3h}, $^3A'_1$)	0	99	2.108	0.256			–0.02755	0.15903
$W_3F_3^+$ (D_{3h}, $^1A'_1$)	0	70	2.362	0.334			–0.47189	0.29245

bridging fluorine atom. The terminal W(1)—F(6) distance is 1.874 Å and is similar to that in monofluorine. The bridging W(1)—F(2)—W(3) distances are little different (2.132 Å vs. 2.084 Å). The lowest heptet state (C_s, $^7A'$) is 0.757 eV above the ground state. As seen from Fig. 1, **1**, the W—F bond length is 2.138 Å for the $W_3F_3^+$ (D_{3h}, $^1A'_1$) cluster. This W—F bond length is lower than the sum (2.90 Å) of covalent W and F radii. The bond length of the planar regular hexagonal $W_3F_3^+$ (D_{3h}, $^1A'_1$) cluster provides the structural criteria of its aromaticity. As seen from Fig. 1, **1**, the W—W bond length $l_{W—W}$ is 2.324 Å for the ground state of $W_3F_3^+$ (D_{3h}, $^1A'_1$) cluster. The bond length $l_{W—W}$ is lower than the sum (2.60 Å) of covalent W and F radii. The bond length of the triangular W_3 framework in the $W_3F_3^+$ (D_{3h}, $^1A'_1$) cluster provides the structural criteria of its aromaticity. The Wiberg bond index (WBI) also provides some information about the existence of ring current. As seen from Table 1, the calculated WBI of W—W for the regular hexagonal $W_3F_3^+$ (D_{3h}, $^1A'_1$) cluster is 2.362, which is between the standard values for double (2.0) and triple (3.0) bonds. This WBI value supports the formation of a delocalized effect on the triangular W_3 framework in the $W_3F_3^+$ (D_{3h}, $^1A'_1$) cluster and therefore the aromatic nature of the $W_3F_3^+$ (D_{3h}, $^1A'_1$) cluster. It goes without saying that the W—W bond of the triangular W_3 framework in the $W_3F_3^+$ (D_{3h}, $^1A'_1$) cluster is a completely delocalized three-center two-electron (3*c*—2*e*) metal-metal bond. The calculated atomic natural electron configuration of W [Xe] $6s^{0.49}5d^{4.48}6p^{0.02}6d^{0.01}7p^{0.11}$of $W_3F_3^+$ (D_{3h}, $^1A'_1$) supports the metal-metal bonding of the W—W interaction.

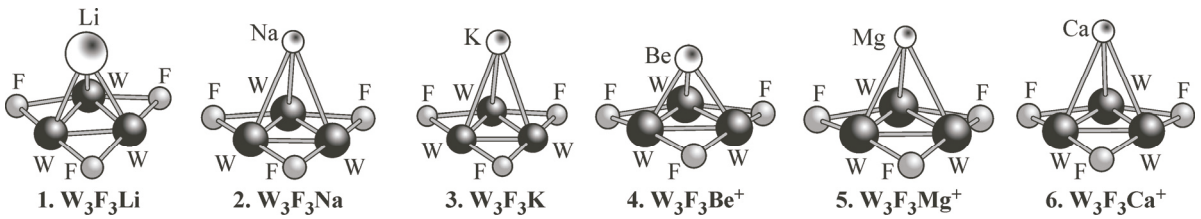

Fig. 2. Optimized structures for the global minimum of the W_3F_3X (X = Li, Na, K) and $W_3F_3Y^+$ (Y = Be, Mg, Ca) all-metal compounds

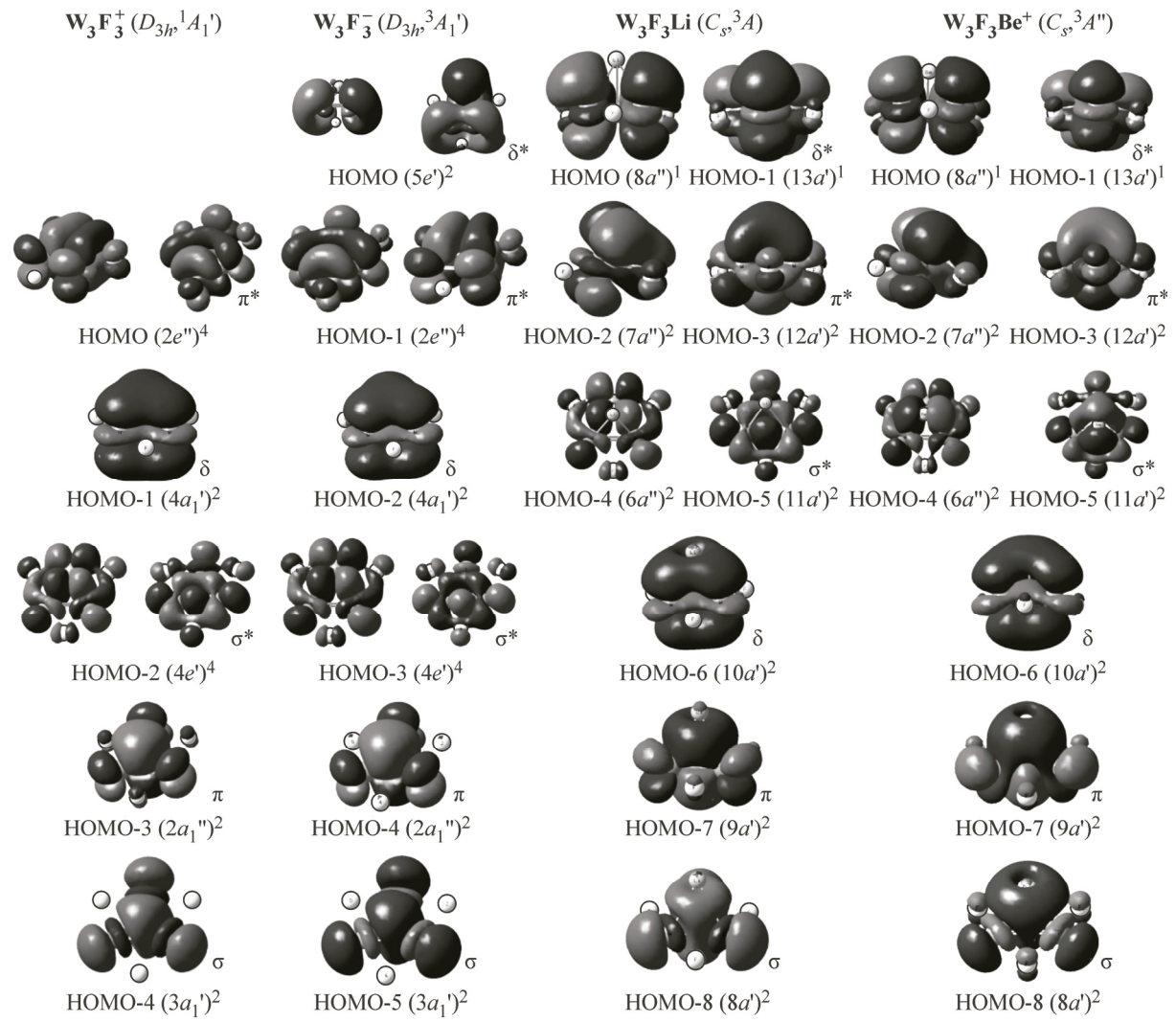

Fig. 3. Seven top MOs in $W_3F_3^+$ (D_{3h}, $^1A_1'$) and nine top MOs in $W_3F_3^-$ (D_{3h}, $^3A_1'$), W_3F_3Li (C_s, $^3A''$), and $W_3F_3Be^+$ (C_s, $^3A''$) responsible for the planar triangular W_3 framework

We also performed an extensive search for the $W_3F_3^-$ global minimum for each spin state at the B3LYP level of theory with the corresponding basis set. For the single charged $W_3F_3^-$ cluster, four geometric isomers were obtained, which had the identical spin state and different symmetry, i.e. structures **8** (D_{3h}, $^3A_1'$), **9** (C_s, $^3A''$), **10** (C_{2v}, $^3B_2$), and **11** (C_1, ^3A), as shown in Fig. 1. Four geometric isomers of $W_3F_3^-$ are minima on the B3LYP potential energy surfaces with all real vibrational frequencies. The theoretical studies show that the $W_3F_3^-$ global minimum has also a planar regular hexagonal structure **8** (Fig. 1) D_{3h} ($^3A_1'$). The energy stability order of the four isomers is **8** = **9** > **10** > **11** at the B3LYP level of theory. The ground state for the $W_3F_3^-$ anion is shown to be a triplet state ($^3A_1'$) with the D_{3h} symmetry. As seen from Fig. 1, the W—F bond length is 2.195 Å for the $W_3F_3^-$ (D_{3h}, $^3A_1'$) anion, which is formed by two electrons from the $W_3F_3^+$ (D_{3h}, $^1A_1'$) cation. The two electrons occupied two doubly degenerate HOMO (5e') bonding/antibonding orbitals. Comparing the perfect D_{3h} structure of $W_3F_3^-$ with that of $W_3F_3^+$, we see that the W—W bond length of $W_3F_3^-$ is slightly longer (0.030 Å) than that of $W_3F_3^+$. This is due to that the additional two electrons occupy the HOMO (5e') of $W_3F_3^-$,

which is an antibonding orbital. The W—F bond length is shorter than the sum (2.90 Å) of covalent radii of W and F atoms. The bond length of the planar regular hexagonal $W_3F_3^-$ (D_{3h}, $^3A_1'$) cluster provides also the structural criteria of its aromaticity. As seen from Table 1, the $WBI_{W—W}$ indices of the $W_3F_3^-$ (D_{3h}, $^3A_1'$) cluster is 2.108, which is between the standard values of double (2.0) and triple (3.0) bonds. This WBI value supports the formation of a delocalized effect on the triangular W_3 framework in the $W_3F_3^-$ (D_{3h}, $^1A_1'$) cluster and therefore the aromatic nature of the $W_3F_3^-$ (D_{3h}, $^3A_1'$) cluster.

MO and chemical bonding analysis. To help understand the electronic structure and bonding nature in the $W_3F_3^{+/-}$ clusters, we carried out a detailed MO and chemical bonding analysis for the $W_3F_3^+$ (D_{3h}, $^1A_1'$) and $W_3F_3^-$ (D_{3h}, $^3A_1'$) ground states (Fig. 3).

Our calculations show that the ground state for $W_3F_3^+$ is a closed shell D_{3h} ($^1A_1'$) structure with a valence electron configuration $1a_1'^2 1e'^4 2a_1'^2 2e'^4 1e''^4 1a_2'^2 3e'^4 1a_2''^2 3a_1'^2 2a_2''^2 4e'^4 4a_1'^2 2e''^4$. Out of the 38 valence electrons in the $W_3F_3^+$ (D_{3h}, $^1A_1'$) cluster, 24 belong to either pure fluorine lone pairs or those polarized towards W responsible for the covalent contributions to the W—F bonding, as in $Hf_3F_3^-$ (D_{3h}, $^1A_1'$) [53]. The remaining 14 valence electrons are primarily W-based and involved in the direct metal-metal bonding. They occupied the top seven MOs of the $W_3F_3^+$ (D_{3h}, $^1A_1'$) cluster (Fig. 3) and are responsible for the perfect triangular W_3 framework. These seven MOs are primarily composed of the 5*d* orbital and partially of W *s*—*p*—*d* hybrid orbitals. For the ground state of $W_3F_3^+$ (D_{3h}, $^1A_1'$) cluster, the fully occupied HOMO-1 ($2e''$) and HOMO-3 ($2a_2''$) form a π bonding/antibonding pair because $2e''$ and $2a_2''$ MOs were composed of totally the same *s*—*p*—*d* hybrid function. They would cancel each other and do not contribute to the net chemical bonding in the $W_3F_3^+$ (D_{3h}, $^1A_1'$) cluster, resulting in negligible metal-metal π bonding. This phenomenon is also observed in the HOMO-4 ($3a_1'$) and HOMO-2 ($4e'$) pair which is, however, a σ_r bonding/antibonding pair. The remaining HOMO ($4a_1'$) is the most important and interesting MO, which is a completely bonding orbital mainly originating from the in-phase overlap of the $5d_{z^2}$ atomic orbital on each W atom perpendicular to the molecular plane. However, this MO perpendicular to the molecular C_3 axis has two nodal surfaces and is symmetric with respect to the molecular plane, thus, it is a δ orbital. The circular delocalization and the bonding nature of the HOMO ($4a_1'$) give rise to δ aromaticity, according to the expanding ($4n$+2) Hückel counting rule. This δ-MO is responsible for the metal-metal bonding and the perfect triangular W_3 framework. It is obvious that the HOMO ($4a_1'$) is a three-center bond (3*c*—2*e*). This low-fluoride transition-metal cluster $W_3F_3^+$ in the $1A_1'$ ($1a_1'^2 1e'^4 2a_1'^2 2e'^4 1e''^4 1a_2'^2 3e'^4 1a_2''^2 3a_1'^2 2a_2''^2 4e'^4 4a_1'^2 2e''^4$) electron state with the D_{3h} symmetry is another example of δ aromaticity in the multinuclear low-fluoride transition metal systems.

Our theoretical results clearly show that the $W_3F_3^-$ anion has a propensity to adopt a triplet $^3A_1'$ state with the D_{3h} symmetry (Table 1). It is predicted that $W_3F_3^-$ is an open-shell structure with a valence electronic configuration $1a_1'^2 1e'^4 2a_1'^2 2e'^4 1a_2'^2 3e'^4 1e''^4 1a_2''^2 3a_1'^2 2a_2''^2 4e'^4 4a_1'^2 2e''^4 5e'^2$. The molecular orbital distribution and the bonding nature in the $W_3F_3^-$ (D_{3h}, $^3A_1'$) anion are totally the same as in the $W_3F_3^+$ (D_{3h}, $^1A_1'$) cation (Fig. 3). Twelve inner shell valence MOs in the $W_3F_3^+$ (D_{3h}, $^1A_1'$) cation were essentially maintained in the $W_3F_3^-$ (D_{3h}, $^3A_1'$) anion since only slight distortions and a change in the orbital order are observed. In the nine top MOs of the $W_3F_3^-$ (D_{3h}, $^3A_1'$) anion, fully occupied HOMO-5 ($3a_1'$) and HOMO-3 ($4e'$) form an σ bonding/antibondiong pair and HOMO-4 ($2a_2''$) and HOMO-1 ($2e''$) form a π bonding/antibonding pair, which should not significantly contribute to the net

aromaticity. The HOMO-2 ($4a'_1$) and HOMO ($5e'$) form a δ bonding/antibonding pair, but the antibonding $5e'$ orbital is half-filled, resulting in a partial δ bonding contribution to the $W_3F_3^-$ (D_{3h}, $^3A'_1$) anion. Thus, the $W_3F_3^-$ (D_{3h}, $^3A'_1$) anion can be considered to possess only a partial δ aromatic character.

The above analysis reveals three types of the *d* bonding interaction existing in the planar regular hexagonal $W_3F_3^+$ (D_{3h}, $^1A'_1$) cation and the $W_3F_3^-$ (D_{3h}, $^3A''_1$) anion. HOMO-4 ($3a'_1$) of the $W_3F_3^+$ (D_{3h}, $^1A'_1$) cation and HOMO-5 ($3a'_1$) of the $W_3F_3^-$ (D_{3h}, $^3A'_1$) anion are the completely delocalized σ-bonding orbital, and HOMO-3 ($2a''_2$) of the $W_3F_3^+$ (D_{3h}, $^1A'_1$) cation and HOMO-4 ($2a''_2$) of the $W_3F_3^-$ (D_{3h}, $^3A'_1$) anion are a completely delocalized π bonding orbital, and HOMO-1 ($4a'_1$) of the $W_3F_3^+$ (D_{3h}, $^1A'_1$) cation and HOMO-2 ($4a'_1$) of the $W_3F_3^-$ (D_{3h}, $^3A'_1$) anion are a completely delocalized δ bonding orbital. Because there are these delocalized bonding orbitals, the Wiberg bond indices (WBIs) of the $W_3F_3^+$ (D_{3h}, $^1A'_1$) cation and the $W_3F_3^-$ (D_{3h}, $^3A''_1$) anion are placed between the standard values of double (2.0) and triple (3.0) bonds.

W_3F_3X (C_s, $^3A''$) (X = Li, Na, K) and $W_3F_3Y^+$ (C_s, $^3A''$) (Y = Be, Mg, Ca). Geometric structure. When one alkali metal cation X^+ ($X^+ = Li^+$, Na^+, and K^+) or one alkaline-earth metal dication Y^{2+} ($Y^{2+} = Be^{2+}$, Mg^{2+}, and Ca^{2+}) approaches a free $W_3F_3^-$ (D_{3h}, $^3A'_1$) anion along the threefold molecular axis, the half-sandwich type W_3F_3X (C_s, $^3A''$) (X = Li, Na, K) or $W_3F_3Y^+$ (C_s, $^3A''$) (Y = Be, Mg, Ca) complexes are produced (Fig. 2). The bond length $l_{W—W}$ = 2.368 ~ 2.368 Å, and 2.366 ~ 2.366 Å, and 2.366 ~ 2.366 Å, $l_{W—F}$ = 2.174 ~ 2.176 Å, and 2.183 ~ 2.185 Å and 2.183 ~ 2.185 Å, for Li, Na, and K, respectively, and the bond length $l_{W—W}$ = 2.419 ~ 2.420 Å, and 2.404 ~ 2.405 Å, and 2.385 ~ 2.386 Å and $l_{W—F}$ = 2.121 ~ 2.122 Å, and 2.139 ~ 2.141 Å and 2.145 ~ 2.149 Å, for Be, Mg, and Ca, respectively. Obviously, $W_3F_3^-$ (D_{3h}, $^3A'_1$) anion structural units were preserved in these half-sandwich type complexes when compared to those in free D_{3h} $(W_3F_3)^-$. This indicates that W—W and W—F interactions are typical completely delocalized single bonds throughout the whole half-sandwich type complex series, and $WBI_{W—W} \approx 1.6$—1.9 and $WBI_{W—F} \approx 0.27$—0.31 were found. $WBI_{W—W}$ (1.6—1.9) is between the standard values of single (1.0) and double (2.0) bonds. It means that there is a ring current effect on the triangular W_3 framework in the $W_3F_3^+$ (D_{3h}, $^1A'_1$) cluster. This WBI value supports the aromatic nature of the $W_3F_3^-$ (D_{3h}, $^3A'_1$) cluster. The X^+—$W_3F_3^-$ and Y^{2+}—$W_3F_3^-$ ionic interactions are clearly demonstrated by the fact that the alkali and alkaline-earth metal atoms in these complexes possess high calculated natural atomic charges Q_{Li} = 0.813|e|, Q_{Na} = 0.805|e|, Q_K = 0.891|e|, and Q_{Be} = 1.152|e|, Q_{Mg} = 1.298|e|, Q_{Ca} = 1.529|e|. The ionicity of these complexes increases from Li to K, Be to Ca, in line with the corresponding total Wiberg bond indices, which decrease from WBI_{Li} = 0.33 to WBI_K = 0.20, and WBI_{Be} = 1.29 to WBI_{Ca} = 0.22. The HOMO energy in the system is effectively lowered from –0.026 eV in free $(W_3F_3)^-$ to –0.222 eV in (W_3F_3Li), and to –0.460 eV in $(W_3F_3Be)^+$, respectively, and the corresponding HOMO-LUMO energy gaps are greater than 0.159 eV in the free $W_3F_3^-$ (D_{3h}, $^3A'_1$) anion. The $W_3F_3^-$ (D_{3h}, $^3A'_1$) anion serves as a robust inorganic ligand in these complexes.

MO and chemical bonding analysis. The structure and bonding in W_3F_3X (C_s, $^3A''$) (X = Li, Na, K) and $W_3F_3Y^+$ (C_s, $^3A''$) (Y = Be, Mg, Ca) can also be understood by analyzing their MOs. As in the $W_3F_3^-$ (D_{3h}, $^3A'_1$) cluster, out of 40 valence electrons in W_3F_3Li (C_s, $^3A''$), 24 belong to either pure fluorine pairs or those polarized towards W (responsible for the covalent contributions to the W—F bonding). The top nine MOs of the free $W_3F_3^-$ (D_{3h}, $^3A'_1$) cluster were essentially maintained in the half-sandwich type W_3F_3Li (C_s, $^3A''$) complex (Fig. 3) since only distortions and a change in the orbital order are observed. The Li center in W_3F_3Li (C_s, $^3A''$) is practically a naked cation. The calculated natural

electron configuration of Li [He] $2s^{0.14}2p^{0.04}$ supports the ionic bonding nature of the Li^+—$W_3F_3^-$ interaction. The Li atom loses its $2s^1$ electron almost completely, whereas its $2p$ orbital remains practically empty (Fig. 3). Similar results exist in the W_3F_3Na and W_3F_3K clusters. An extensive calculation results shows that the ground state of W_3F_3Li is a C_s ($^3A''$) structure with a valence electronic configuration $1a'^21a''^22a'^23a'^24a'^22a''^23a''^25a'^24a''^25a''^26a'^27a'^28a'^29a'^210a'^211a'^26a''^212a'^27a''^213a'^18a''^1$. As shown in Fig. 3, the $11a'$ and $6a''$ MOs of W_3F_3Li (C_s, $^3A''$) are two antibonding σ* MOs, which mainly originate from the two degenerate $4e'$ MOs of free $W_3F_3^-$ (D_{3h}, $^3A_1'$) and $8a'$ MO of W_3F_3Li (C_s, $^3A''$) is a completely delocalized σ bonding MO, which mainly originate from $3a_1'$ MO of free $(W_3F_3)^-$ (D_{3h}, $^3A_1'$). The fully occupied $8a'$ and $11a'$, $6a''$ MOs of W_3F_3Li (C_s, $^3A'$) form a σ bonding/antibonding pair and do not contribute to the chemical bonding in W_3F_3Li (C_s, $^3A''$). The $7a''$ and $12a'$ MOs of W_3F_3Li (C_s, $^3A''$) mainly originate from the bonding/antibonding doubly degenerate $2e''$ MOs of free $W_3F_3^-$ (D_{3h}, $^3A_1'$), this two MOs of W_3F_3Li (C_s, $^3A''$) are a bonding/antibonding pair π* MOs, and $9a'$ MO of W_3F_3Li (C_s, $^3A''$) mainly originate from $2a_2''$ of free $W_3F_3^-$ (D_{3h}, $^3A_1'$), $9a'$ is a completely delocalized π bonding MO. The $9a'$ and $7a''$, $12a'$ orbitals form a π bonding/antibonding pair, but the antibonding $8a''$ (HOMO) orbital is half-filled, resulting in a partial π bonding contribution to W_3F_3Li (C_s, $^3A''$). Analogously, the $10a'$ and $12a'$, $13a'$ MOs form a δ bonding/antibonding pair, the same half-filled $13a'$ orbital results in partial δ bonding in W_3F_3Li (C_s, $^3A''$). It is these delocalized partial δ bonding MOs that render the local ring-current effects to the W_3 triangles, and therefore, aromaticity of the $W_3F_3^-$ ligands in these half-sandwich type complexes. In $W_3F_3Y^+$ (C_s, $^3A''$) (Y = Be, Mg, Ca) complexes, alkaline-earth metal centers possess the natural atomic configurations of Be[He] $2s^{0.57}2p^{0.27}3d^{0.01}$, Mg[Ne] $3s^{0.63}3p^{0.06}3d^{0.01}$, Ca[Ar] $4s^{0.26}3d^{0.21}$, respectively. In these complexes, alkaline-earth metal centers lose most of their ns^2 electrons, whereas their np or $(n-1)d$ orbitals gain only a small portion back from the $W_3F_3^-$ ligands. The low occupations of the valence np or $(n-1)d$ atomic orbitals indicate that covalent p—d or d—d interactions contribute slightly to the overall bonding of the systems. The calculation results show that $W_3F_3Be^+$ (C_s, $^3A''$) and W_3F_3Li (C_s, $^3A''$) are an open-shell C_s ($^3A_1''$) structure with same valence electronic configuration $1a'^21a''^22a'^23a'^24a'^22a''\times$ $\times^23a''^25a'^24a''^25a''^26a'^27a'^28a'^29a'^210a'^211a'^26a''^212a'^27a''^213a_1'^18a''^1$ since only slight distortions are observed, because $W_3F_3Be^+$ (C_s, $^3A''$) and W_3F_3Li (C_s, $^3A''$) are valence isoelectronic species, therefore, $W_3F_3Be^+$ (C_s, $^3A''$) also possesses a partial δ-aromatic character (Fig. 3). Similarly, the delocalized σ, π, and δ bonding orbitals in the half-sandwich type W_3F_3Li (C_s, $^3A''$) and $W_3F_3Be^+$ (C_s, $^3A''$) complexes have also led to an increase in their $WBI_{W—W}$.

CONCLUSIONS

Extensive DFT calculations are performed in search for the lowest energy structures of multinuclear low-fluoride transition metal $W_3F_3^{+/-}$ clusters and their half-sandwich type W_3F_3X (C_s, $^3A''$) (X = Li, Na, K) and $W_3F_3Y^+$ (C_s, $^3A''$) (Y = Be, Mg, Ca) complexes. The ground state of the $W_3F_3^+$ cation is a D_{3h}, $^1A_1'$ ($1a_1'^21e'^42a_1'^22e'^41e''^41a_2'^23e'^41a_2''^23a_1'^22a_2''^24e'^44a_1'^22e''^4$) structure that possesses three types of the d orbital chemical bonding and gives rise to δ aromaticity and the ground state of the $W_3F_3^-$ anion is a D_{3h}, $^3A_1'$ ($1a_1'^21e'^42a_1'^22e'^41a_2'^23e'^41e''^41a_2''^23a_1'^22a_2''^24e'^44a_1'^22e''^45e'^2$) structure which also possesses three types of the d orbital chemical bonding and gives rise to partial δ aromaticity. The results obtained from the present work are another example for low-fluoride transition metal clusters containing δ aromaticity. The half-sandwich type W_3F_3X (C_s, $^3A''$) (X = Li, Na, K) and $W_3F_3Y^+$ (C_s, $^3A''$) (Y = Be, Mg, Ca) complexes containing partial δ aromatic ligands can be provided. These novel complexes may be used in future experiments to open a new field of coordination chemistry.

REFERENCES

1. *Schleyer P.v.R., Jiao H.* // Pure. Appl. Chem. – 1996. – **68**. – P. 209.
2. *Li X., Kuznetsov A.E., Zhang H.F., Boldyrev A.I., Wang L.S.* // Science. – 2001. – **291**. – P. 859.
3. *Kuznetsov A.E., Boldyrev A.I., Li X., Wang L.S.* // J. Am. Chem. Soc. – 2001. – **123**. – P. 8825.
4. *Kuznetsov A.E., Corbet J.D., Wang L.S., Boldyrev A.I.* // Angew. Chem. Int. Ed. – 2001. – **40**. – P. 3369.
5. *Li X., Zhang H.F., Wang L.S., Kuznetsov A.E., Cannon N.A., Boldyrev A.I.* // Angew. Chem. Int. Ed. – 2001. – **40**. – P. 1867.
6. *Boldyrev A.I., Kuznetsov A.E.* // Inorg. Chem. – 2002. – **41**. – P. 532.
7. *Kuznetsov A.E., Boldyrev A.I., Zhai H.J., Li X., Wang L.S.* // J. Am. Chem. Soc. – 2002. – **124**. – P. 11791.
8. *Kuznetsov A.E., Boldyrev A.I.* // Struct. Chem. – 2002. – **13**. – P. 141.
9. *Alexandrova A.N., Boldyrev A.I.* // J. Phys. Chem. A. – 2003. – **107**. – P. 554.
10. *Yong L., Chi X.X.* // J. Mol. Struct. (THEOCHEM.) – 2007. – **818**. – P. 93.
11. *Alexandrova A.N., Boldyrev A.I., Zhai H.J., Wang L.S.* // J. Chem. Phys. – 2005. – **122**. – P. 054313-1.
12. *Ma J., Li Z., Fan K., Zhou M.* // Chem. Phys. Lett. – 2003. – **372**. – P. 708.
13. *Li Q.S., Jin Q.* // J. Phys. Chem. A. – 2003. – **108**. – P. 855.
14. *Li Q.S., Jin Q.* // J. Phys. Chem. A. – 2003. – **107**. – P. 7869.
15. *Li Q.S., Gong L.F.* // J. Phys. Chem. A. – 2004. – **108**. – P. 4322.
16. *Alexandrova A.N., Zhai H.J., Wang L.S., Boldyrev A.I.* // Inorg. Chem. – 2004. – **43**. – P. 3552.
17. *Boldyrev A.I., Wang L.S.* // Chem. Rev. – 2005. – **105**. – P. 3716.
18. *Xu W.G., Zhang Y.C., Xi Q.* // J. Mol. Struct. (THEOCHEM.) – 2009. – **909**. – P. 129.
19. *Xu W.G., Zhang R.C., Lu S.X., Zhang Y.C.* // J. Mol. Struct. (THEOCHEM.) – 2009. – **894**. – P. 1.
20. *Jin Q., Jin B., Xu W.G.* // J. Mol. Struct. (THEOCHEM.) – 2005. – **713**. – P. 113.
21. *Jin Q., Jin B., Xu W.G.* // Chem. Phys. Lett. – 2004. – **396**. – P. 398.
22. *Xu W.G., Jin B.* // Chem. Phys. Lett. – 2006. – **419**. – P. 439.
23. *Xu W.G., Jin B.* // J. Mol. Struct. (THEOCHEM.) – 2006. – **759**. – P. 101.
24. *Xu W.G., Jin B.* // J. Mol. Struct. (THEOCHEM.) – 2005. – **731**. – P. 61.
25. *Tsipis C.A.* // Coord. Chem. Rev. – 2005. – **249**. – P. 2740.
26. *Hofmann M.* // Heteroat. Chem. – 2006. – **17**. – P. 224.
27. *Zubarev D.Y., Averkiev B.B., Zhai H.J., Wang L.S., Boldyrev A.I.* // Phys. Chem. Chem. Phys. – 2008. – **10**. – P. 257.
28. *Kuznetsov A.E., Corbet J.D., Wang L.S., Boldyrev A.I.* // Angew. Chem. Int. Ed. – 2001. – **40**. – P. 3369.
29. *Alexandrova A.N., Boldyrev A.I., Zhai H.J., Wang L.S.* // J. Phys. Chem. A. – 2005. – **109**. – P. 562.
30. *Huang X., Zhai H.J., Kiran B., Wang L.S.* // Angew. Chem. Int. Ed. – 2005. – **44**. – P. 7251.
31. *Zhai H.J., Averkiev B.B., Zubarev D.Y., Wang L.S., Boldyrev A.I.* // Angew. Chem. Int. Ed. – 2007. – **46**. – P. 4277.
32. *Alexandrova A.N., Boldyrev A.I., Zhai H.J., Wang L.S.* // Coord. Chem. Rev. – 2006. – **250**. – P. 2811.
33. *Averkiev B.B., Boldyrev A.I.* // J. Phys. Chem. A. – 2007. – **111**. – P. 12864.
34. *Cotton F.A., Curtis N.F., Harris C.B., Johnson B.F.G., Lippard S.J., Mague J.T., Robinson W.R., Wood J.S.* // Science. – 1964. – **145**. – P. 1305.
35. *Yong L., Wu S.D., Chi X.X.* // Int. J. Quantum. Chem. – 2007. – **107**. – P. 722.
36. *Chi X.X., Liu Y.* // Int. J. Quantum. Chem. – 2007. – **107**. – P. 1886.
37. *Wang B., Zhai H.J., Huang X., Wang L.S.* // J. Phys. Chem. A. – 2008. – **112**. – P. 10962
38. *Huang X., Zhai H.J., Kiran B., Wang L.S.* // Angew. Chem. Int. Ed. – 2005. – **44**. – P. 7251.
39. *Zhai H.J., Wang B., Huang X., Wang L.S.* // J. Phys. Chem. A. – 2009. – **113**. – P. 9804.
40. (a) *Zhai H.J., Wang B., Huang X., Wang L.S.* // J. Phys. Chem. A. – 2009. – **113**. – P. 3866. (b) *Chen W.J., Zhai H.J., Zhang Y.F., Huang X., Wang L.S.* // J. Phys. Chem. A. – 2010. – **114**. – P. 5958.
41. *Feng X.J., Cao T.T., Zao L.X., Lei Y.M., Luo Y.* // Eur. Phys. J. D. – 2008. – **50**. – P. 285.
42. *Alvarado-Soto L., Ramírez-Tagle R., Arratia-Pérez R.* // Chem. Phys. Lett. – 2008. – **467**. – P. 94.
43. *Sergeeva A.P., Boldyrev A.I.* // Comm. Inorg. Chem. – 2010. – **31**. – P. 2.
44. *Alvarado-Soto L., Ramírez-Tagle R., Arratia-Pérez R.* // J. Phys. Chem. A. – 2009. – **113**. – P. 1671.
45. *Li S., Zhai H.J., Wang L.S., Dixon D.A.* // J. Phys. Chem. A. – 2009. – **113**. – P. 11273.
46. *Zhai H.J., Wang L.S.* // Chem. Phys. Lett. – 2010. – **500**. – P. 185.
47. *Lin S.J., Zhan X.H., Xu L., Wang B., Zhang Y.F., Huang X.* // J. Phys. Chem. A. – 2013. – **117**. – P. 3093.
48. *Frisch M.J., Trucks G.W., Schlegel H.B. et al.* Gaussian 03. Revision C.01. Gaussian., Inc., Pittsburgh PA., 2003.
49. *Becke A.D.* // J. Chem. Phys. – 1993. – **98**. – P. 5648.
50. *Lee C., Yang W., Parr R.G.* // Phys. Rev B. – 1988. – **37**. – P. 785.
51. *Perdew J.P., Wang Y.* // Phys. Rev B. – 1992. – **45**. – P. 13244.
52. *Reed A.E., Curtiss L.A., Weinhold F.* // Chem. Rev. – 1988. – **88**. – P. 899.
53. *Jin B., Jin Q.* // Comput. Theor. Chem. – 2013. – **1013**. – P. 130.